Germany, June 5 - 10, 2005

INDUCTION PERIOD OF HETEROGENEOUS NUCLEATION DURING CRYSTALLISATION FOULING: ION IMPLANTATION EFFECTS

G. Rizzo [1], H. Müller-Steinhagen[2] and E. Richter[3]

[1] Institute of Thermodynamics and Thermal Engineering, University of Stuttgart, Pfaffenwaldring 6, D-70550 Stuttgart, Germany, e-mail: rizzo@itw.uni-stuttgart.de

[2] Institute of Thermodynamics and Thermal Engineering, University of Stuttgart, Pfaffenwaldring 6, D-70550 Stuttgart, Germany, e-mail: hms@itw.uni-stuttgart.de

[3]Institute of Ion Beam Physics and Materials Research, FZ Rossendorf e.V., Postfach 51 01 19, D-01314 Dresden, Germany, e-mail: e.richter@fz-rossendorf.de

ABSTRACT

In this paper the influence of the surface properties on heterogeneous nucleation of calcium sulphate hemihydrate is investigated. While the roughness of the investigated stainless steel samples was kept constant, the surface properties were varied by direct ion implantation of fluorine, oxygen, hydrogen and neon. The completed fouling tests show that the induction periods of the fluorine and oxygen implanted surfaces were consistently longer than those for the untreated ones, with fluorine implantation producing the longest induction times. On the other hand, the hydrogen and especially the neon ion implanted samples showed significantly shorter induction times than the untreated surfaces. Unfortunately this trend could not be correlated with calculated surface energies measured by the sessile drop contact angle method. The heterogeneous nucleation was determined by plotting ln (induction period) vs. $\ln^{-2}$ (supersaturation ratio), where the supersaturation ratio was varied from 1.65 to 2. A linear relationship between the slope of the heterogeneous nucleation curves and the electro-negativity of the implanted ions was discovered. Furthermore, a clear change-over from mass transfer controlled to reaction controlled fouling can be identified during variation of the flow velocity between 0.125 and 0.200 m/s - i.e. Reynolds numbers between 5400 and 11442. Additionally, it can be clearly seen that the surface properties in the case of mass transfer controlled fouling have less influence than for reaction controlled crystal deposition.

INTRODUCTION

Fouling is still one of the crucial remaining problems in the practical use of heat exchangers. In particular it causes a reduction in thermal efficiency and an increase of pressure drop. To compensate this, oversizing and/or redundant equipment are common practice. Also additional maintenance is normally required to keep the plant capacity constant. The overall annual costs due to heat exchanger fouling are estimated to be 0.25 % of the gross domestic product (GDP) in highly industrialized countries (Steinhagen et al., 1993).

Until now the mechanisms of fouling – i.e. the build-up of unwanted depositions on the heat transfer surfaces – are not exactly known. In general it is assumed (Epstein, 1983), that in all types of fouling the events: initiation, migration, attachment, transformation or aging occur sequentially and parallel to them removal or re-entrainment take place. In the case of crystallisation fouling the initial step is unambiguously the heterogeneous nucleation process. If it would be possible to prevent nucleation or to decrease the nucleation rate, then the prevention of scaling or at least an extension of the time until a closed crystalline cover appears is possible.

For technical reasons it is important to know the time span until a noticeable change in heat transfer occurs and how intense this change will be. Even a few crystal layers are able to decrease the overall heat transfer coefficient due to their usually low thermal conductivity. However the first crystals do not necessarily reduce heat transfer. They generally increase the surface roughness and hence the local film heat transfer coefficients. If this contribution is higher than the reduction due to their additional heat conduction resistance, the overall heat transfer coefficient can become even higher than the clean one (Müller-Steinhagen, 2002). Therefore, the time from the beginning of the heat transfer process until the moment at which the overall heat transfer changes is defined - in this paper - as the induction time of heterogeneous crystal nucleation. A typical fouling resistance vs. time curve is shown in Fig. 1.

The induction period during crystallisation fouling is mainly influenced by the degree of supersaturation, the characteristics of the liquid/solid interface and the properties of the crystalline material. To explore the impact of the nucleating wall, it is necessary to vary separately the different

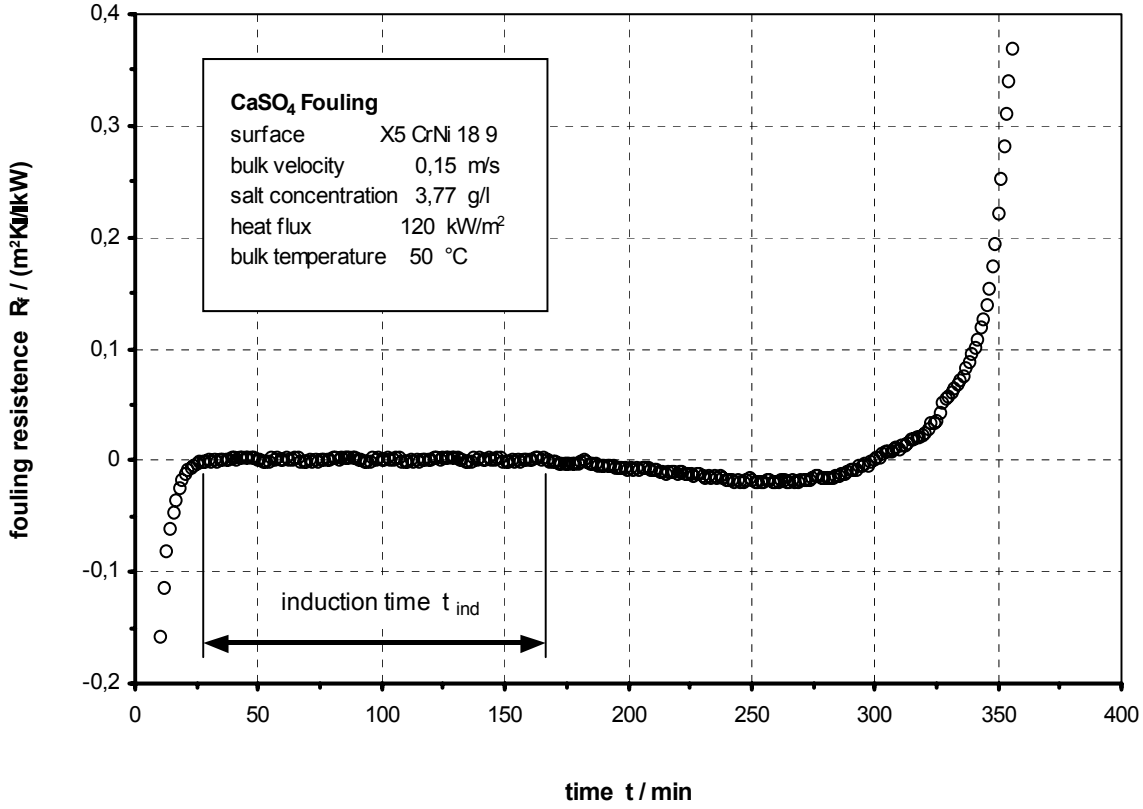

Fig. 1 : Definition of induction period – as used in this investigation

surface properties, while keeping supersaturation and crystal type constant. Förster (2001) thoroughly investigated the influence of surface macro-roughness of stainless steel samples on the induction time during calcium sulphate fouling. He also had a look at surface chemistry. Unfortunately he was not able to maintain the surface roughness of the different materials at constant values. Zettler et al. (2005) were confronted with the same problem, when they investigated the influence of surface properties on crystallisation fouling in a plate-and-frame heat exchanger. The influence of wall temperature and bulk velocity on fouling in a 1.83 m long stainless steel tube which was heated from the outside with a constant uniform heat flux was recently investigated by Fahiminia et al. (2003).

However, surface characteristics do not only influence the initiation of fouling, the whole fouling process will be affected as well (Müller-Steinhagen and Zhao, 1997; Bornhorst et al., 1999; Müller-Steinhagen et al., 2000). The more nuclei exist, the more crystals will grow and the quicker they will interlink with each other. As soon as contact is established, their undisturbed growth will be constrained and a fine-grained structure will appear. In addition to this, the adherence of the deposit to the wall will be influenced by the surface properties (Packham, 1992) and hence the suitability for cleaning (Boulangé-Petermann et al., 2003).

THEORETICAL BACKGROUND

According to the classical nucleation theory (Volmer and Weber, 1926), nuclei will immediately appear as soon as a certain supersaturation is achieved. This very first moment is however difficult to detect. The sizes of nuclei in a supersaturated aqueous salt solution are in the range of nanometers. Therefore the nuclei first have to grow to a crystal of certain size before they are detectable. On the other hand some assumptions were made in the classical theory, which can not be exactly fulfilled in reality. For example, a certain time is required until the system is in a quasi-steady-state and stable nuclei are able to be formed.

In this investigation the signal to detect the appearance of fouling is the change in heat transfer or fouling resistance, see Fig. 1. It is hence obvious, that the induction period t_{ind} has to be inversely proportional to the rate of nucleation J and the growth rate R of the crystals. The more nuclei are initiated the faster a surface will be covered, and the faster this first crystal layer is growing the sooner a significant additional heat transfer resistance appears.

By applying classical nucleation theory (Chernov, 1984) the rate of nucleation under homogeneous nucleation conditions is

$$J = B \cdot \exp\left[- \frac{16 \pi v^2 \gamma_{SL}^3}{3 k^3 T^3 \ln^2(S)} \right] \quad (1)$$

assuming that the nuclei are spherical. Here, the growth parameter v is defined as

$$v = \frac{M}{N_A \cdot \rho_C} \quad . \quad (2)$$

Since $t_{ind} \propto 1/J$, the induction time will be

$$\ln(t_{ind}) \propto \frac{16 \pi v^2 \gamma_{SL}^3}{3 k^3 T^3} \cdot \ln^{-2}(S) \quad . \quad (3)$$

From Eq. (3) it can be clearly seen that the slope of the curve $\ln(t_{ind})$ vs. $\ln^{-2}(S)$ is mainly dependent on the interfacial tension γ_{SL} between the nuclei and the salt solution and on the solution temperature (Mullin, 2001). For a heterogeneous nucleation process the classical theory yields

$$J = B \cdot \exp\left[- \frac{(1-\cos\Theta)^2 \cdot (2+\cos\Theta)}{4} \cdot \frac{16 \pi v^2 \gamma_{SL}^3}{3 k^3 T^3 \ln^2(S)} \right] \quad (4)$$

(Chernov, 1984) and thus

$$\ln(t_{ind}) \propto \frac{(1-\cos\Theta)^2 (2+\cos\Theta)}{4} \cdot \frac{16 \pi v^2 \gamma_{SL}^3}{3 k^3 T^3} \ln^{-2}(S) \quad (5)$$

Comparing Eq. (3) and Eq. (5) a noticeable change in the slope of the nucleation curves should appear if heterogeneous instead of homogeneous nucleation occurs. Since the factor

$$\frac{(1-\cos\Theta)^2 \cdot (2+\cos\Theta)}{4} \quad (6)$$

is always between 0 and 1, the slope of the heterogeneous curve will always be less than that of the homogenous one. Experimentally this effect was first observed by Söhnel and Mullin (1978), while studying $CaCO_3$ precipitation at 25° C, as can be seen in Fig. 2. If the surface is fully covered by a spreading monomolecular crystal layer (i.e. $\Theta = 0$), Eq. (4) will change into Eq. (1) and hence the induction time will be the same for a heterogeneous and a homogenous nucleation process.

Furthermore, it is possible to predict the interfacial tension γ_{SL} at equilibrium solubility following a fundamental derivation by Mersmann (2001)

$$\gamma_{SL} = 0.414 \cdot kT \cdot \left(\frac{\rho_c N_A}{M} \right)^{\frac{2}{3}} \cdot \ln\left(\frac{c_S}{c_L} \right) \quad . \quad (7)$$

These facts together with the knowledge of the slope of experimental data drawn in a $\ln(t_{ind})$ vs. $(\ln^{-2}(S)$ plot enables one to distinguish whether the nucleation process was homogenous or heterogeneous.

Much less is known about the influence of crystal growth rate on the induction period. As soon as stable nuclei are formed, they will immediately start to grow. The crystal growth will continue as long as the supersaturation is present. Several theories concerning the growth rate have been postulated. Each of them explained a special experimental observation. In general, all of the reported mechanisms can be broadly discussed under three headings: surface energy theories, diffusion theory or adsorption-layer theory (Mullin, 2001). In the field of heat exchanger fouling the diffusion theory is common (Bott, 1995).

$$\dot{m}_t = \beta \cdot A \cdot (c_B - c^*). \quad (8)$$

$$\dot{m}_r = K \cdot A \cdot (c^* - c_S)^n. \quad (9)$$

$$c^* = c_S \Rightarrow \dot{m} = \beta \cdot A \cdot (c_B - c_S). \quad (10)$$

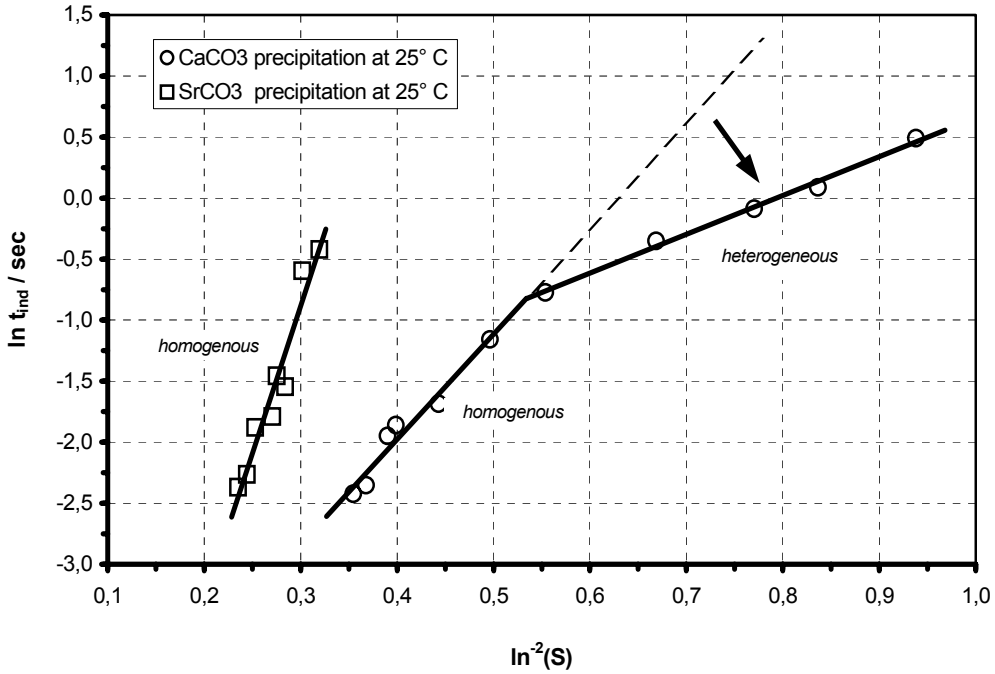

Fig. 2 : The change in the slope indicates a transition from homogenous to heterogeneous nucleation (Data from Söhnel and Mullin, 1978)

EXPERIMENTAL PROCEDURE

All presented results were obtained from fouling experiments in a closed loop set-up with two identical test sections, which were operated in parallel. The complete experimental rig is made of stainless steel, except for the connections to the pump, which are out of EPDM, a chemical resistant rubber, which was used to separate the vibrations of the pump from the set up. A schematic diagram of the test rig is shown in Fig. 3. The actual test sections are two rectangular ducts with a side ratio of 3:1, in which the long sides is 39 mm. They are installed vertically. On both wide sides of each duct an opening of 59 mm by 50 mm exist, where the samples were mounted. The samples were heated from the back by infrared radiators over an area of 40 mm by 20 mm (whereby the long side is in line with the duct axis). The heated zone is positioned 80 hydraulic diameters downstream from the inlet of the ducts. This means, that the hydraulic flow is fully developed, while thermal developing conditions exist. During all experiments the heat flux was equal to 120,000 W/m^2 and the wall temperature was kept constant at 97 °C. To achieve these parameters, the bulk temperature had to be suitably adjusted. In Fig. 4 a cross-section of the sample holder including the IR radiators and a view on the flow channel is depicted. The wall temperature was measured with thermocouples placed in a copper block, which is vacuum-soldered to the backside of each sample. The registered temperatures were corrected by the corresponding temperature drop to the channel inside wall value. In the same copper block a second thermocouple was installed, with a distance of 12.5 mm from the first one. In this way it was possible to measure the heat flux via the temperature drop. A closed loop controller with an electronic dimmer adjusted the transferred heat flux and kept it constant.

The supersaturated fouling fluid was prepared by mixing an aqueous calcium nitrate tetrahydrate ($Ca(NO_3) \cdot 4\ H_2O$) solution with an aqueous sodium sulphate (Na_2SO_4) solution in such a way that the desired $CaSO_4$ concentration was finally available. The two chemicals were dissolved separately in 23.5 litres of demineralised water and heated up to the final bulk temperature. Immediately after mixing, the calcium concentration of the final solution was measured by potentiometric EDTA titration and visually controlled so that no turbidity occurred. In addition to the visual observation a 12 µm pore filter was installed to ensure that no suspended crystals flowed past the heated samples. Since the final fouling solution contains in addition to hydrated calcium and sulphate ions also hydrated potassium and nitrate ions the equilibrium solubility of calcium sulphate and its hydrates is changed due to the so-called "salting effect" (Marshall et al., 1964). Therefore, at the investigated wall temperature of 97 °C calcium sulphate hemihydrate will be most probably precipitating. This assumption is also supported by the Osswald rule of stages (Mullin, 2001).

The temperature of the bulk solution was measured by a thermocouple at the inlet to the test sections and adjusted by another closed loop with three band heaters and a cooling coil.

The surfaces examined in this paper were all of basic material stainless steel AISI 304 BA, ion implanted with fluorine, oxygen, hydrogen and neon. The ion implantations were done by direct ion bombardment. Since different ions

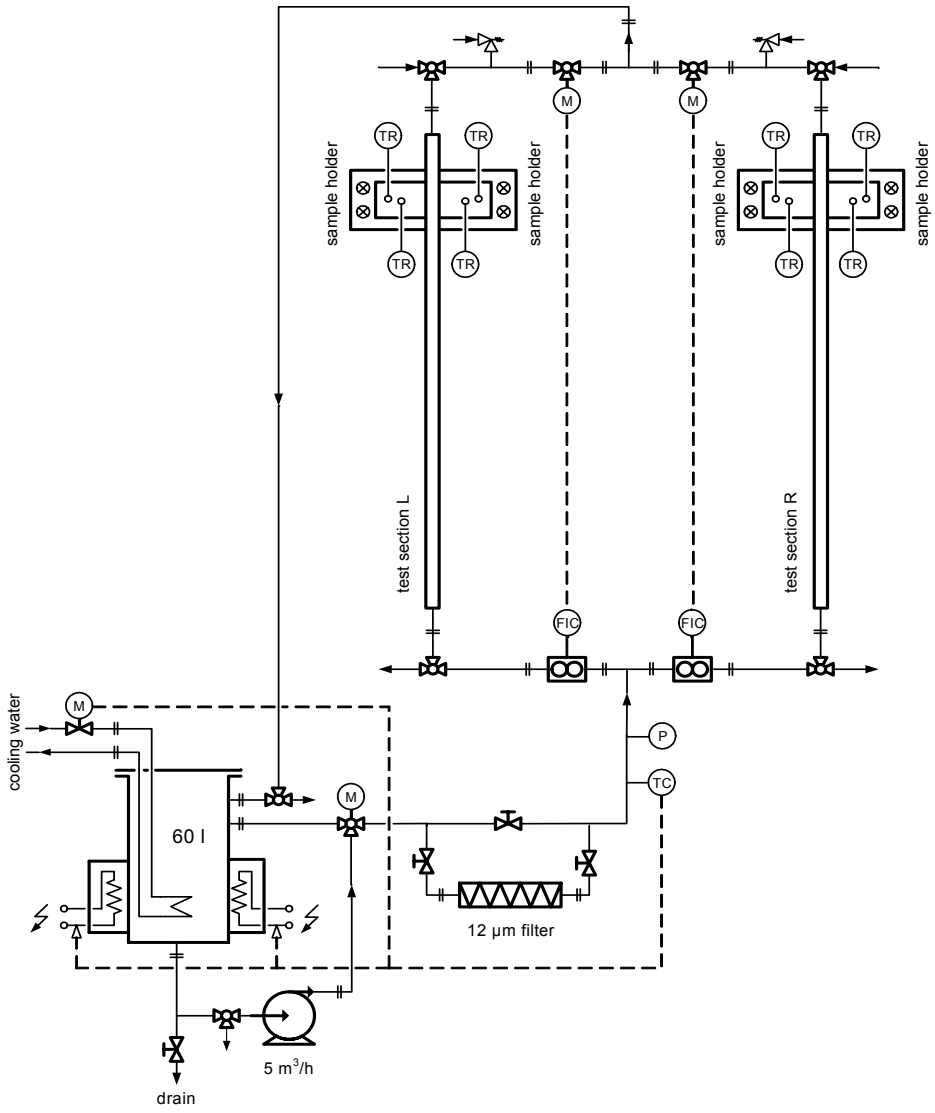

Fig. 3 : Flow chart of the experimental set-up.

settle down in different depths (Ziegler et al., 1985), it was necessary to adjust the implantation energies, so that the concentration maximum of the diverse ions will have the same distance to the surface. With the aid of the simulation program TRIM[1] (Transport of Ions in Matter) it was possible to calculate the ion concentration distribution perpendicular to the surface, as shown in Fig. 5 for fluorine. As can be seen the concentration maximum lies at a depth of 171.8 nm. To realize the same maximum depth and a similar contour of the concentration distribution for all kinds of implanted ions, the corresponding implantation energies and doses have to be chosen, as listed in Table 1.

A crucial problem for investigating the influence of surface chemistry on the induction period during crystallisation fouling is how to keep the surface roughness constant. In most cases the microscopic as well as the macroscopic roughness will change when the surface is modified. The only way to solve this problem is to roughen the samples after the ion implantation process. Superfinishing pads of grain size 30 µm (A40 according to ANSI) were used in combination with a double rotating sanding process (Dubbel and Grote, 2005). In this way, it was guaranteed that even minor surface topography changes which may have happened during the ion implantation will be removed. The surface roughness of the investigated samples was measured with a stylus instrument (Perthometer M4Pi, Mahr, Germany) over a length of 5.8 mm in three different directions, and was characterized by different surface texture parameters.

[1] Calculations were performed with SRIM-2003 version 20 (see www.SRIM.org).

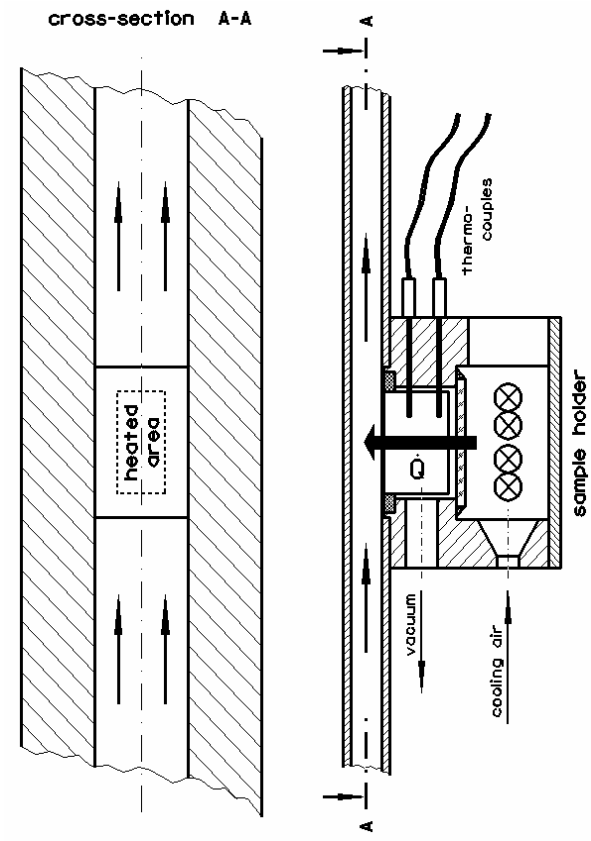

Fig. 4 : Cross-section of sample holder and flow channel.

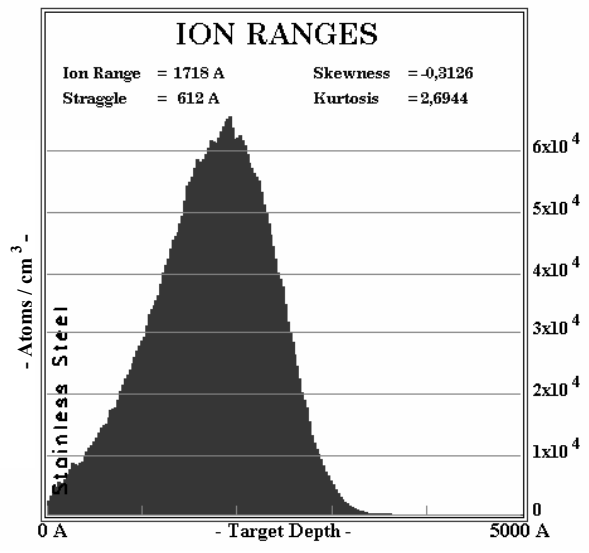

Fig. 5 : Calculated fluorine ion concentration perpendicular to the surface by TRIM

Table 1: Ion implantation energies and dose of the implanted ions

Ion	Energy	Dose
	keV	*ions/cm²*
fluorine	186,00	$5 \cdot 10^{16}$
oxygen	176,40	$5 \cdot 10^{16}$
hydrogen	29,40	$5 \cdot 10^{16}$
neon	200,00	$5 \cdot 10^{16}$

After the sanding process the samples were cleaned twice with toluene and installed immediately after. Then the test rig was powered up with demineralised water until a steady state was reached. As soon as the wall temperature became stable for more than one hour, the water was removed and replaced by the test solution. After another ten minutes, the heating was turned on and the experiment started. Altogether 21 runs were carried out, whereby the concentration of the solution was varied between 3.31 and 3.96 g_{CaSO_4} / ltr_{H_2O}. This means for a wall temperature of 97 °C and the deposition of calcium sulphate hemihydrate, that the supersaturation ratio was between 1.65 and 2 (Marshall et al., 1964). In addition, the bulk velocity was changed to 0.125, 0.150, 0,175 and 0.200 m/s for the oxygen implanted, the neon implanted and the unmodified sample.

RESULTS AND DISCUSSION

Influence of fluid velocity. To define adequate experimental conditions where the influence of surface chemistry can be explicitly seen, it was necessary to know the velocity range where the effect of mass transfer on fouling is negligible. Therefore, the bulk velocity was varied from 0.125 m/s up to 0.200 m/s. These primary tests were done with the oxygen and the neon ion implanted samples as well as with an untreated one. The resulting induction periods vs. the velocity are shown in Fig. 6 for a salt concentration of 3.51 g_{CaSO_4} / ltr_{H_2O}.

In general it can be said that the surface modifications influence the induction period over the whole investigated velocity range, even though at low velocities this effect is much smaller than at velocities higher than 0.150 m/s. The reason for this trend has to be – according to diffusion theory (Bott, 1995) – the changing mass transfer. The incorporation of matter into the crystal lattice, described mathematically by a chemical reaction, was constant for all investigated velocities, since surface temperature, heat flux and supersaturation were kept constant. A change-over from mass transfer controlled to reaction controlled fouling takes place while the velocity is increased. The same tendency was found by Fahiminia et al. (2003) for the induction period during calcium sulphate fouling in a circular tube. There the change-over took place approximately at 0.5 m/s and was much steeper, most likely because of other experimental conditions.

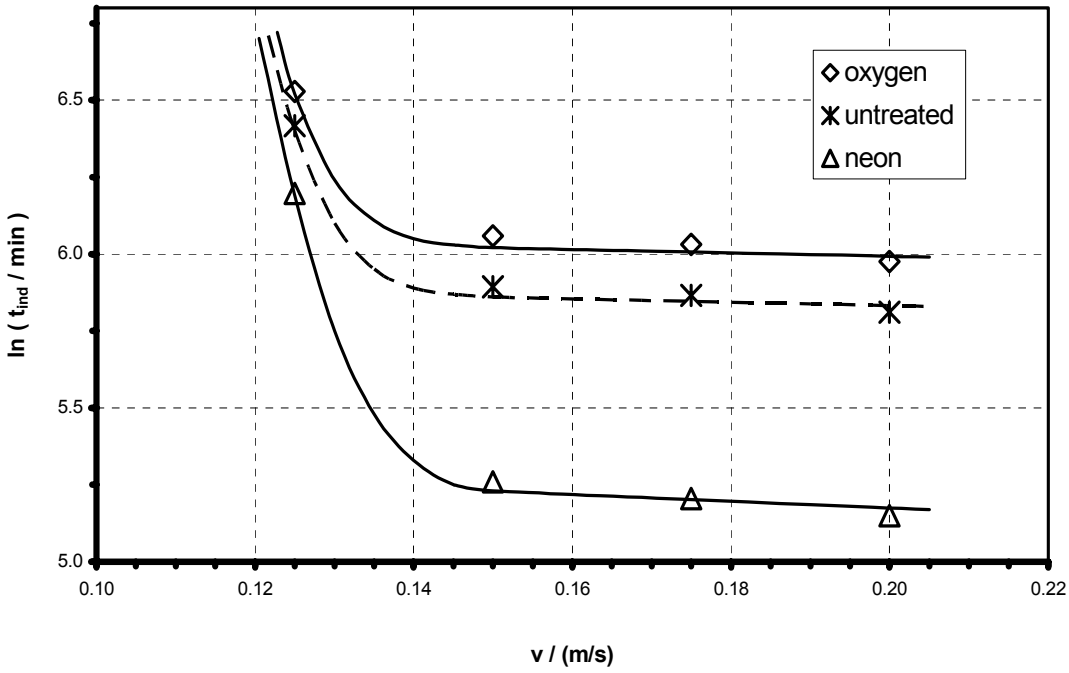

Fig. 6 : Development of the induction period vs. bulk velocity for different ion implantations (c = 3.51 g_{CaSO4} / ltr_{H2O}).

Thus, to perform meaningful fouling tests which show explicitely the effect of surface properties on the induction time, bulk velocities higher than 0.150 m/s have to be determined. But even in doing so, the induction period will still be influenced by the velocity (see Fig. 6 velocities > 0.150 m/s). Theoretically one has to choose an infinitely high velocity to measure the pure influence of surface property on the induction period. Unfortunately high fluid velocities require high bulk temperatures in order to reach the desired wall temperature. On the other hand, the higher the fouling fluid temperature the more probable ~~is~~ a sudden bulk precipitation of calcium sulphate from the highly supersaturated experimental solution will be. To consider both limitations a compromise has to be made. Because of the practical reasons mentioned before, a fluid velocity of 0.150 m/s was chosen, for all the following experiments.

Influence of surface chemistry. At first, three sets of freshly sanded stainless steel samples were examined to check the reproducibility of results. As can be seen in Fig. 7 the data points for untreated surfaces are, for the same supersaturation, close to each other and the effect of supersaturation can be approximated by a straight line in a double-logarithmic diagram.

Thus it can be concluded that the two test sections are working identically and that the reproducibility of the results is assured. According to Eq. (3) the slope of the curve $\ln(t_{ind})$ vs. $\ln^{-2}(S)$ in the case of homogenous nucleation is

$$\frac{d(\ln(t_{ind}))}{d(\ln^{-2}(S))} = \frac{16\,\pi\,v^2\gamma_{SL}^3}{3\,k^3T^3} \quad . \qquad (11)$$

This means that in the case of bulk precipitation of calcium sulphate hemihydrate a theoretical slope of 431.08 ln(min) should be expected. The straight line for untreated surfaces in Fig. 7, however, rises with a slope of only 1.646 ln(min). It indicates that heterogeneous nucleation occurs on the heat transfer surfaces over the complete investigated range of supersaturation and that no bulk precipitation followed by particle fouling takes place. In the case of the ion implanted samples different slopes were recognized, see Fig. 8. While the line-fits through the experimental results with fluorine and oxygen implantation are steeper than the untreated ones, the hydrogen and especially the neon ion implanted samples show significantly shorter induction times. The reason for these observations are, according to theory (Eq. (1) to Eq. (5)), the different interfacial energies, because the foulant and its surface tension were the same for all the samples and experiments.

Surface characterization. The surface roughness of the investigated samples is described by different surface texture parameters (DIN EN ISO 4287). Since the sanding procedure and the used grain size were the same for all samples, only the average value is given in Table 2. The roughness parameters were measured in three different directions as indicated in Fig. 9.

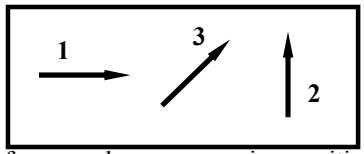

Fig. 9: Surface roughness measuring positions and directions

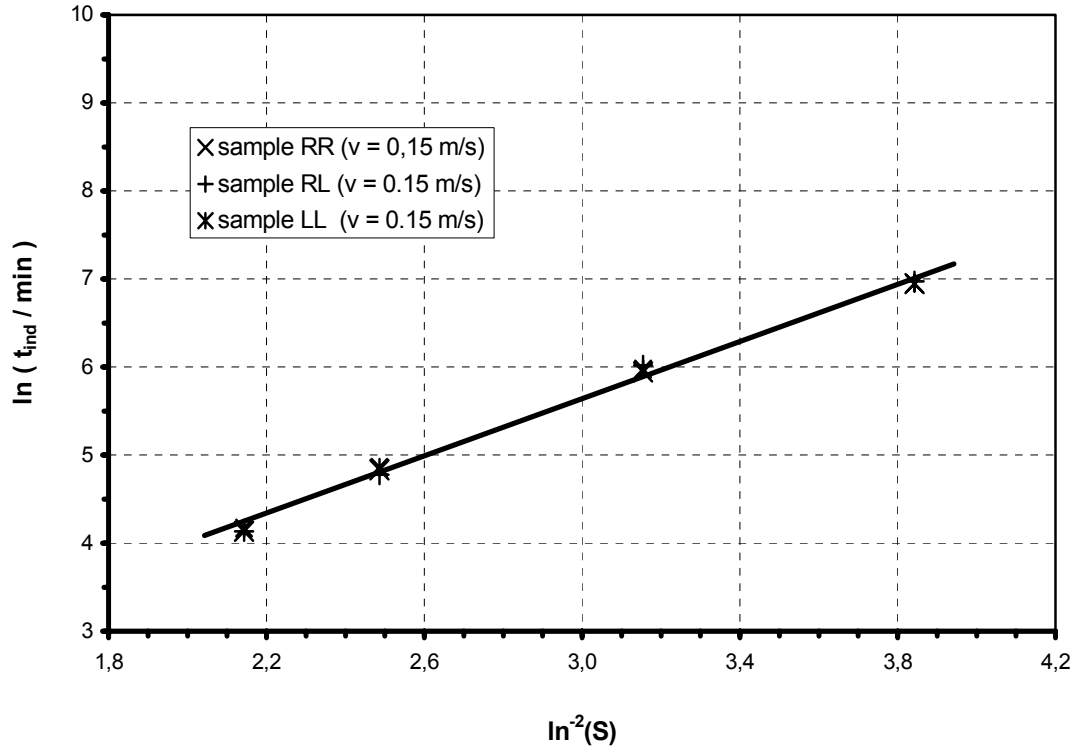

Fig. 7 : Nucleation behaviour of untreated samples

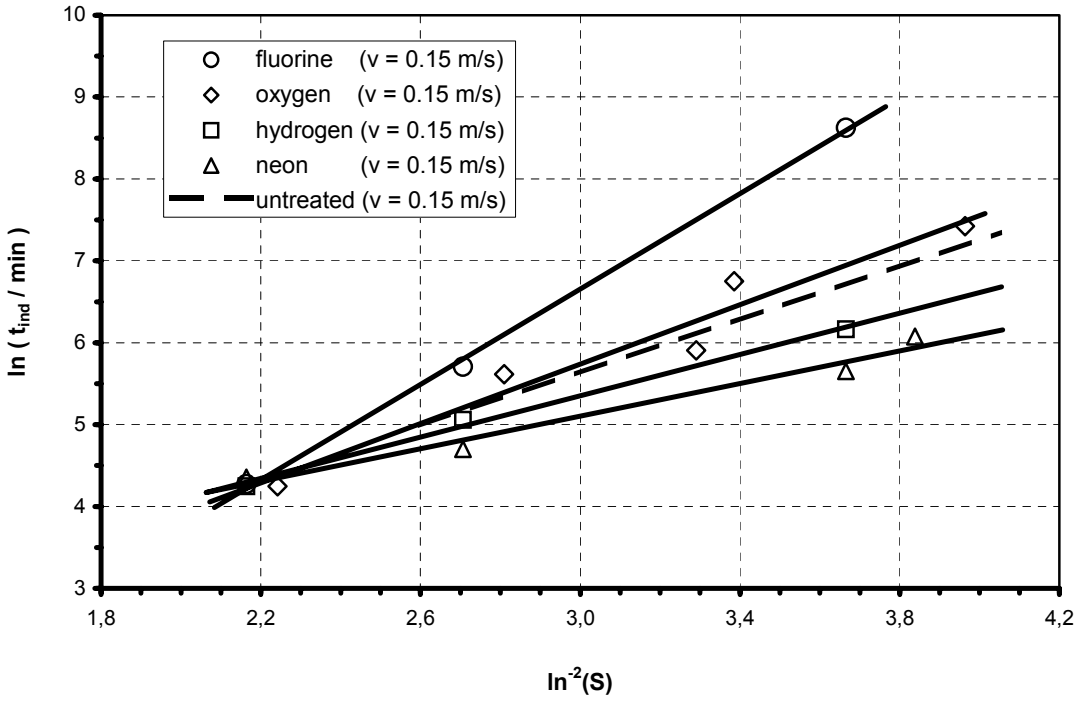

Fig. 8 : Nucleation behaviour of fluorine, oxygen, hydrogen and neon implanted samples

Table 2 : Surface roughness characterised by surface texture parameters according to DIN EN ISO 4287 (sampling length 5.8 mm/cut-off wave 0.8 mm)

parameter	R_a	R_q	R_z	R_{3z}	R_t	R_{max}	R_p	R_{pk}	R_k	R_{vk}	Mr_1	Mr_2
direction	µm	µm	µm	µm	µm	µm	µm	µm	µm	µm	µm	µm
1	0,14	0,20	1,09	0,70	1,53	1,43	0,54	0,20	0,35	0,53	12,6 %	81,2 %
2	0,13	0,16	0,84	0,61	1,09	1,03	0,46	0,15	0,43	0,23	14,3 %	86,6 %
3	0,15	0,20	1,15	0,73	1,51	1,46	0,56	0,24	0,36	0,51	13,0 %	80,2 %

As can be seen from Eq. (1) – Eq. (5) the interfacial energy has a very strong influence on the heterogeneous nucleation process. Since in all examined fouling tests the foulant was always the same, i.e. calcium sulphate hemihydrate, the variation in interfacial energy has to be attributed to the different surface tensions of the investigated heat transfer surfaces. To analyse the results shown in Fig. 7 and 8 the surface energies measured by the sessile drop method and calculated by different theories are presented in Fig. 10 - 12. Unfortunately, no unique relationship between the measured induction periods and the surface energies could be identified, neither for the total nor for the different components of the surface energy. No conclusive explanation can be given for this, to-date.

Another way to characterise the examined surfaces is through the properties of the implanted ions. The basic material was in all cases stainless steel AISI 304 BA. Into this material different ions were implanted. The depth of the implantation maximum was exactly the same. Thus the final surface property was changed in a definite direction according to the properties of the corresponding ion. Since the concentrations of the implanted ions are very low – it was impossible to detect them by EDX – it can be assumed that the contribution of the ions to the van der Waals and the polar forces, and consequently to the

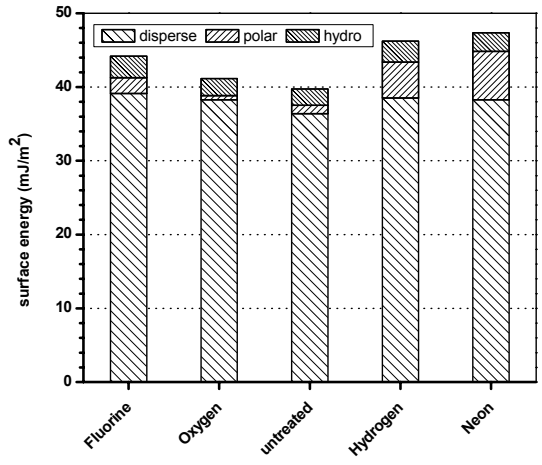

Fig. 10 : Surface energies of the ion implanted samples calculated by the enhanced Fowkes theory (Chen and Wakida, 1997)

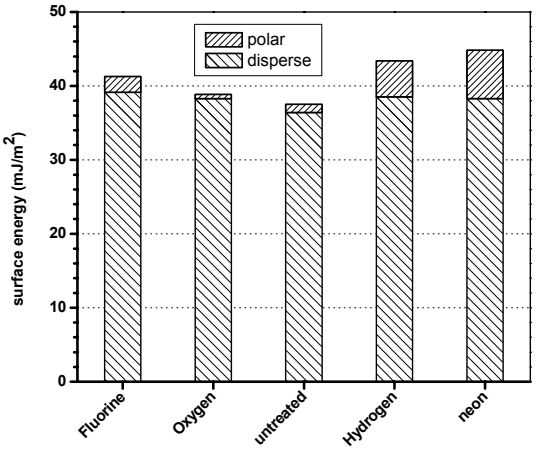

Fig. 11 : Surface energies of the ion implanted samples calculated according to OWENS, WENDT, RABEL, KAELBLE (Owens and Wendt, 1969)

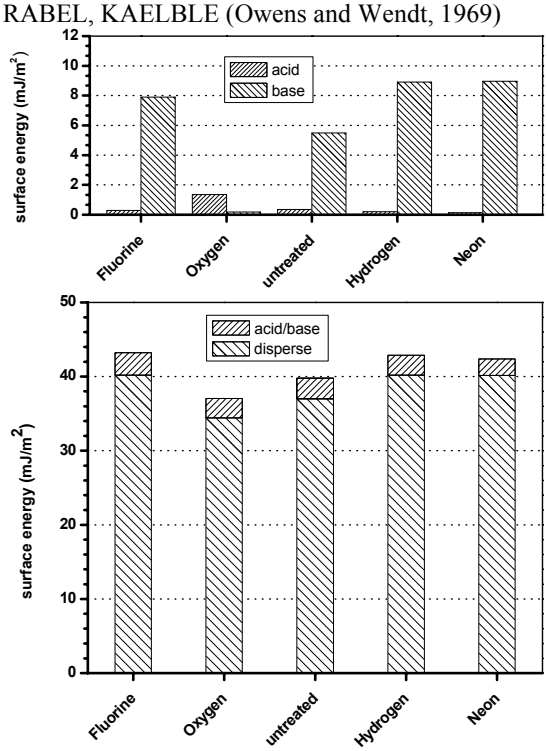

Fig. 12 : Surface energies of ion implanted samples calculated according to VAN OSS (1994)

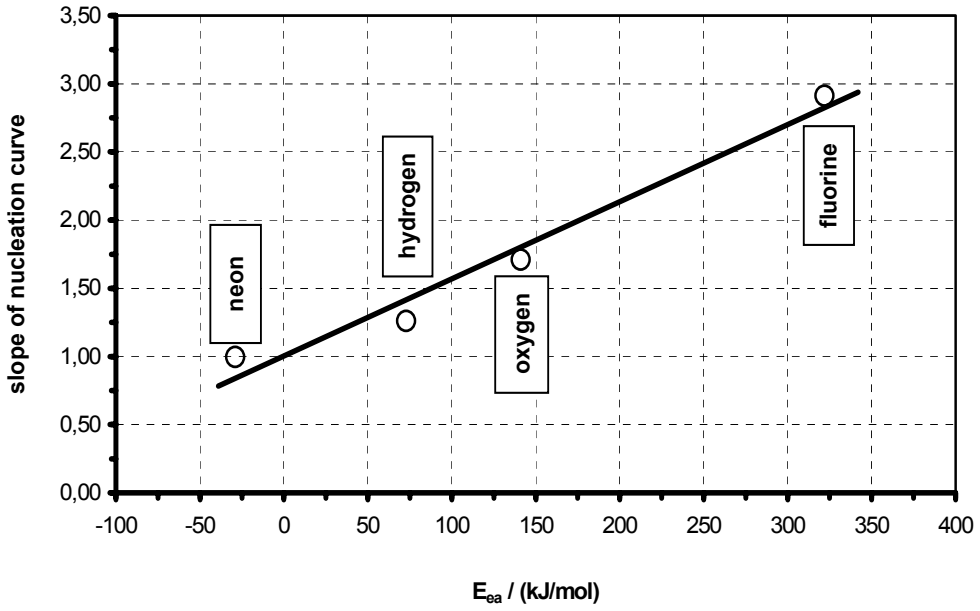

Fig. 13 : Slope of nucleation curves vs. electro-negativity E_{ea} of fluorine, oxygen, hydrogen and neon ions

overall interfacial tension, can be negligible. The only possible effect the implanted ions are able to have is the creation of active sites. The reactivity of such sites is normally described by the Lewis acid/base theory. Here, an acid is defined as a surface group which is able to accept an electron and a base is able to deliver electrons (Atkins and De Paula, 2002). This ability is very much correlated to the electronegativity, i.e. the bonding strength of an electron to an ion. The stronger an ion is attracting its electrons, the higher the probability that it will behave like an acid. If the ion tends to releasing its electrons, it will show basic properties. The contribution of Lewis acid/base surface sites to the interfacial energy can be up to one magnitude higher than the van der Waals forces (Visser, 1998). Therefore, the measured slope of the $\ln(t_{ind})$ vs. $\ln^{-2}(S)$ curves were plotted as a function of electronegativity of the implanted ions. It is obvious, that there is a strong correlation between these two values, as can be seen in Fig. 13, which may be approximated by a straight line.

CONCLUSION

It has been shown that primary heterogeneous nucleation occurs on the heat transfer surface over the whole investigated range of supersaturation. The induction period of the nucleation process

1. depends strongly on the fluid velocity as long as mass transfer has a significant impact. At velocities higher than 0.15 m/s the initial fouling stage becomes mainly reaction controlled and the influence of the velocity may be neglected. In this parameter range surface chemistry becomes essential.
2. is only at lower supersaturations noticeably influenced by the surface properties. At high supersaturation, the difference in the induction period is less dependent on surface chemistry. At a supersaturation ratio of approximately 2 the induction time of all ion implantations becomes equal.
3. could not be correlated with results of surface tension measurements, as would have been expected from theory. Instead, a linear relation between the slope of the ln (induction period) vs. $\ln^{-2}$ (supersaturation ratio) nucleation plots and the electronegativity of the implanted ions was observed.

ACKNOWLEDGMENT

The authors would like to acknowledge Prof. Jamialahmadi from the University of Petroleum Industry, Ahwaz/Iran for his helpful discussions during his visit to the University of Stuttgart. In addition, the authors would like to thank Dr. Ziegler for providing the stopping range simulation program SRIM for calculating the distribution of the implanted ions.

NOMENCLATURE

A	Area	m^2
B,C	constants	-
c	solute concentration	$kmol / m^3$
J	nucleation rate	$1 / (s\ m^2)$
k	Boltzmann constant	$1.38 \cdot 10^{-23}$ J / K
M	molar mass	kg / kmol
m	mass flow rate	kg / s

N_A	Avogadro constant	$6.022 \cdot 10^{26}$ 1 / kmol
n	order of reaction	-
R	growth rate	kg / s
S	supersaturation ratio	c / c_s
T	temperature	K
t	time	s

Superscript

*	outer surface of the stagnant film

Subscript

B	bulk	
C	crystal	
L	liquid	
S	solid	
r	reaction	
s	saturation	
t	mass transport	
β	mass transfer coefficient	m / s
γ	surface energy	J / m^2
ρ	density	kg / m^3
θ	contact angle	rad

REFERENCES

Atkins, P., De Paula, J., 2002: *Physical Chemistry.* 7th ed., Oxford University Press, Oxford.

Bornhorst, A, Zhao, Q. and Müller-Steinhagen, H., 1999: Reduction of Scale Formation by Ion Implantation and Magnetron Sputtering on Heat Transfer Surfaces. *Heat Transfer Engineering*, vol. 20, no. 2, pp. 6 – 14.

Bott, T.R. 1995: *Fouling of Heat Exchangers*. Elsevier, Amsterdam.

Boulangé-Petermann, L., Debacq, C., Poiret, P., Cromieres, B., 2003: Effect of the physical chemistry of polymeric coating surfaces on fouling and cleanability with particular reference to the food industry. In *Contact Angle, Wettability and Adhesion*, ed. by Mittal, K.L., vol. 3, VSP, Utrecht.

Chen, J.-R. and Wakida, T., 1997: Studies on surface free energy and surface structure of PTFE film treated with low temperature plasma. *Journal of Applied Polymer Science,* vol. 63, pp. 1733 – 1739.

Chernov, A.A., 1984: *Modern Crystallography III: Crystal Growth*. Springer, Berlin.

Dubbel, H. and Grote, K.-H., 2005: *Taschenbuch für den Maschinenbau*. 21th ed., Springer, Berlin.

Epstein, N., 1983: Thinking about Heat Transfer Fouling: A 5 x 5 Matrix. *Heat Transfer Engineering*, vol. 4, no. 1, pp. 43 – 56.

Fahiminia, F., Watkinson, A.P. and Epstein, N., 2003: Investigation of Initial Fouling Rates of Calcium Sulphate Solutions under Non-boiling Conditions. *ECI Conference on Heat Exchanger Fouling and Cleaning: Fundamentals and Applications*. Santa Fé, New Mexico, USA (see http://services.bepress.com/eci/heatexchnager/1/).

Förster, M.L., 2001: Verminderung des Kristallisationsfoulings durch gezielte Beeinflussung der Grenzfläche zwischen Kristallen und Wärmeübertragungsfläche. *PhD Thesis*, Cuvillier, Göttingen.

Marshall, W.L., Slusher, R. and Jones, E.V., 1964: Aqueous Systems at High Temperatures. *Journal of Chemical Engineering Data*, vol. 9, no. 2. pp. 187 – 191.

Mersmann, A.: *Crystallization technology handbook*. 2nd ed., Dekker, New York.

Müller-Steinhagen, H., 2002: Verschmutzung von Wärmeübertragerflächen. In *VDI Wärmeatlas*, 9th ed., Springer, Berlin.

Müller-Steinhagen, H. and Zhao, Q., 1997: Investigation of low fouling surface alloys made by ion implantation technology. *Chemical Engineering Science*, vol. 52, no. 19, pp. 3321 – 3332.

Müller-Steinhagen, H., Zhao, Q., Helali-Zadeh, A. and Ren, X.-G., 2000: The Effect of Surface Properties on CaSO4 Scale Formation during Convective Heat Transfer and Subcooled Flow Boiling. *The Canadian Journal of Chemical Engineering*, vol. 78, pp. 12 – 20.

Mullin, J.W., 2001: Crystallization. 4th ed., Butterworth-Heinemann, Oxford.

Owens, D.K. and Wendt, R.C., 1969: Estimation of the Surface Free Energy of Polymers. *Journal of Applied Polymer Science,* vol. 13, pp. 1741 – 1747.

Packham, D.E., 1992: *Handbook of Adhesion*. Longman Scientific & Technical, Harlow.

Söhnel, O. and Mullin, J.W., 1978: A method for determination of precipitation induction period. *Journal of Crystal Growth*, vol. 44, pp. 377 – 382.

Steinhagen, R., Müller-Steinhagen, H. and Maani, K., 1993: Problems and Costs due to Heat Exchanger Fouling in New Zealand Industries. *Heat Transfer Engineering*, vol. 14, no. 1, pp. 19 – 30.

Valeton, J.J.P., 1923: Wachstum und Auflösung der Kristalle. *Zeitschrift für Kristallographie*, vol. 59, pp. 335 – 365.

Van Oss, C.J., 1994: *Interfacial Forces in Aqueous Media*. Dekker, New York.

Visser, H., 1998: The Role of Surface Forces in Fouling of Stainless Steel in the Dairy Industry. *Journal of Dispersion Science and Technology*, vol. 19, no. 6 & 7, pp. 1127 – 1150.

Volmer, M. and Weber, A., 1926: Keimbildung in übersättigten Gebilden. *Zeitschrift für physikalische Chemie*, vol. 119, pp. 277 – 301.

Zettler, H.U., Weiß, M., Zhao, Q. and Müller-Steinhagen, H., 2005: Influence of Surface Properties and Characteristics on Fouling in Plate Heat Exchangers. *Heat Transfer Engineering*, vol. 26, no. 2, pp. 3 – 18.

Ziegler, J.F., Biersack J.P. and U. Littmark, U., 1985: *The Stopping and Range of Ions in Solids*. Pergamon Press, New York.